Supporting Information

Out-of-Plane Transient Thermal Conductivity Measurements for Bulk Semiconducting Conjugated Polymers using Fast Scanning Calorimetry

Haoyu Zhao[a], Nathaniel Prine[a], Guorong Ma[a], Yongcao Zhang[b], Md Azimul Haque[b], Derya Baran[b] and Xiaodan Gu[a]*

[a]School of Polymer Science and Engineering, The University of Southern Mississippi, Hattiesburg, MS 39406, United States of America

[b]Physical Sciences and Engineering Division, KAUST Solar Center, King Abdullah University of Science and Technology, Thuwal, 23955, Saudi Arabia

E-mail: xiaodan.gu@usm.edu

This file includes:

Figure S1 to S14

Table S1 to S3

Discussion related to our technique

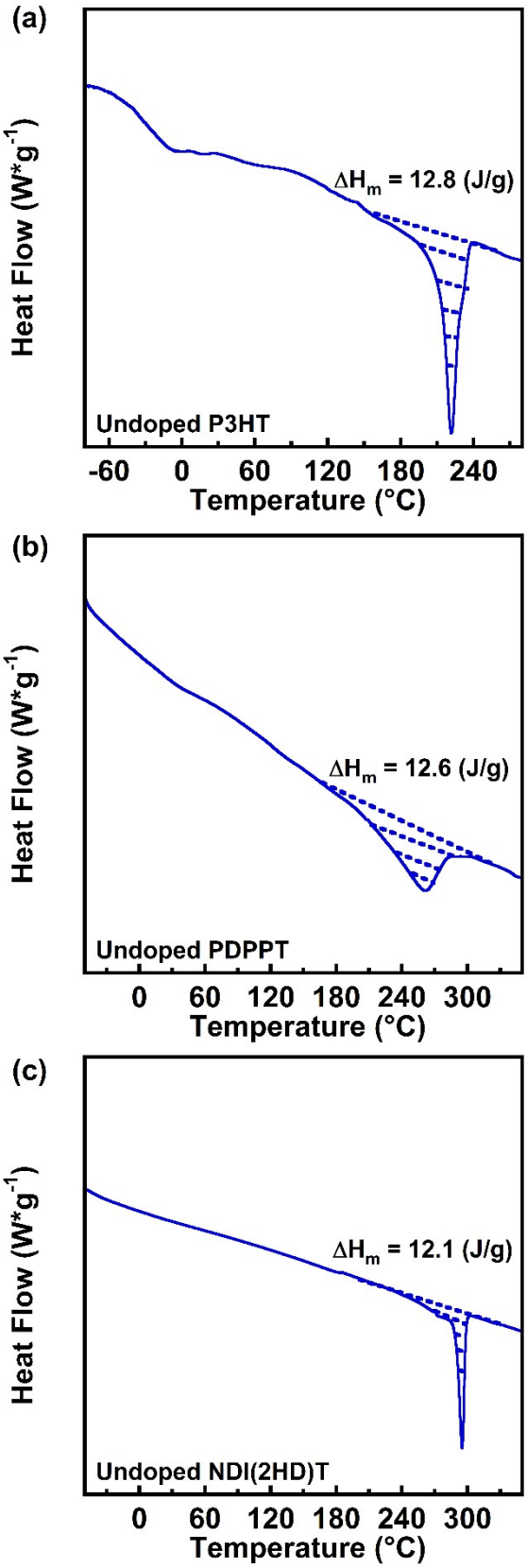

Figure S1. Representative conventional DSC scans for **a)** undoped P3HT **b)** undoped PDPPT **c)** undoped NDI(2HD)T specific heat capacity measurements

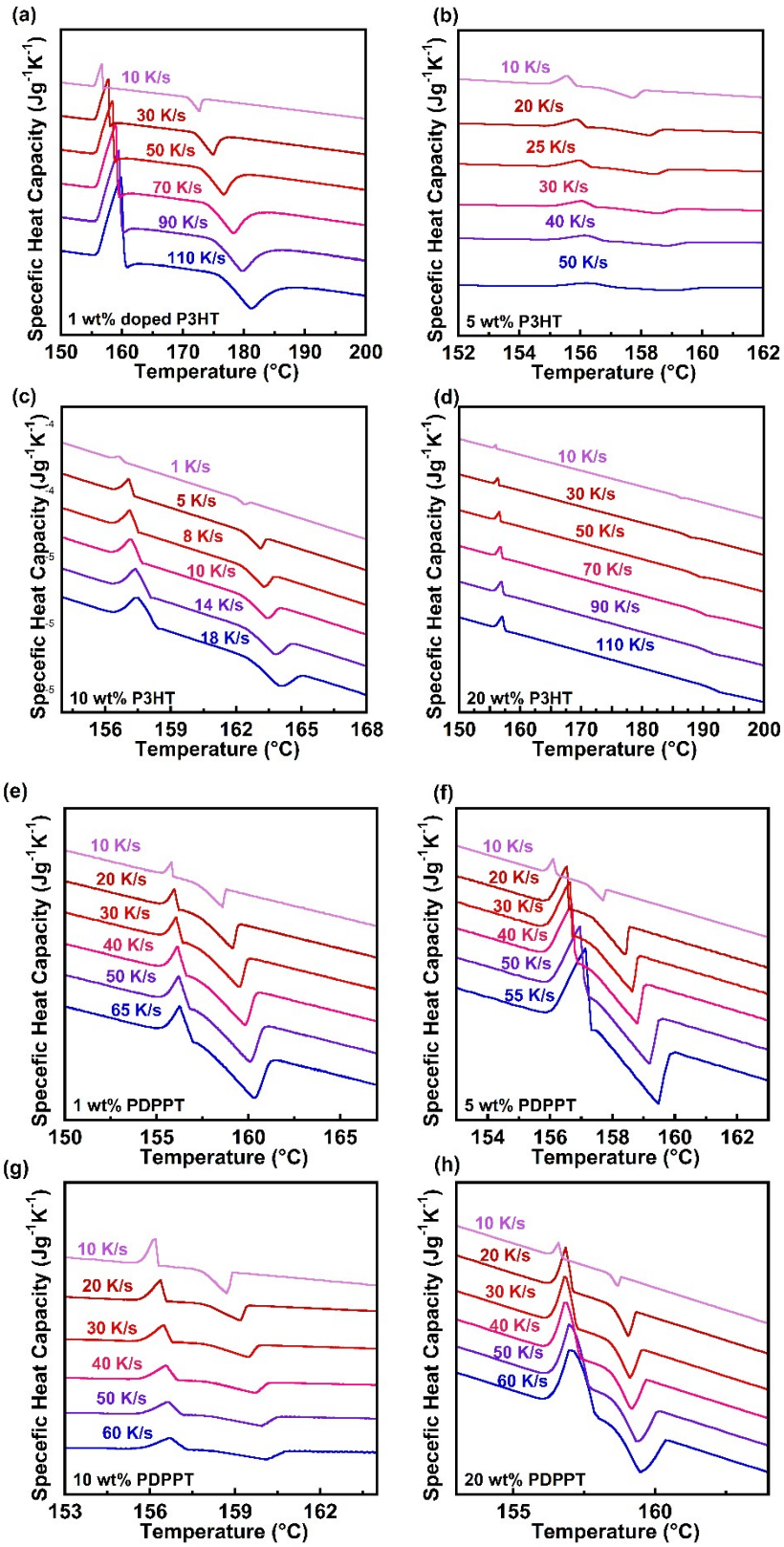
(a)
Specefic Heat Capacity (Jg-1K-1)
10 K/s
30 K/s
50 K/s
70 K/s
90 K/s
110 K/s
1 wt% doped P3HT
150 160 170 180 190 200
Temperature (°C)
(b)
Specefic Heat Capacity (Jg-1K-1)
10 K/s
20 K/s
25 K/s
30 K/s
40 K/s
50 K/s
5 wt% P3HT
152 154 156 158 160 162
Temperature (°C)
(c)
Specefic Heat Capacity (Jg-1K-1)
1 K/s
5 K/s
8 K/s
10 K/s
14 K/s
18 K/s
10 wt% P3HT
156 159 162 165 168
Temperature (°C)
(d)
Specefic Heat Capacity (Jg-1K-1)
10 K/s
30 K/s
50 K/s
70 K/s
90 K/s
110 K/s
20 wt% P3HT
150 160 170 180 190 200
Temperature (°C)
(e)
Specefic Heat Capacity (Jg-1K-1)
10 K/s
20 K/s
30 K/s
40 K/s
50 K/s
65 K/s
1 wt% PDPPT
150 155 160 165
Temperature (°C)
(f)
Specefic Heat Capacity (Jg-1K-1)
10 K/s
20 K/s
30 K/s
40 K/s
50 K/s
55 K/s
5 wt% PDPPT
154 156 158 160 162
Temperature (°C)
(g)
Specefic Heat Capacity (Jg-1K-1)
10 K/s
20 K/s
30 K/s
40 K/s
50 K/s
60 K/s
10 wt% PDPPT
153 156 159 162
Temperature (°C)
(h)
Specefic Heat Capacity (Jg-1K-1)
10 K/s
20 K/s
30 K/s
40 K/s
50 K/s
60 K/s
20 wt% PDPPT
155 160
Temperature (°C)

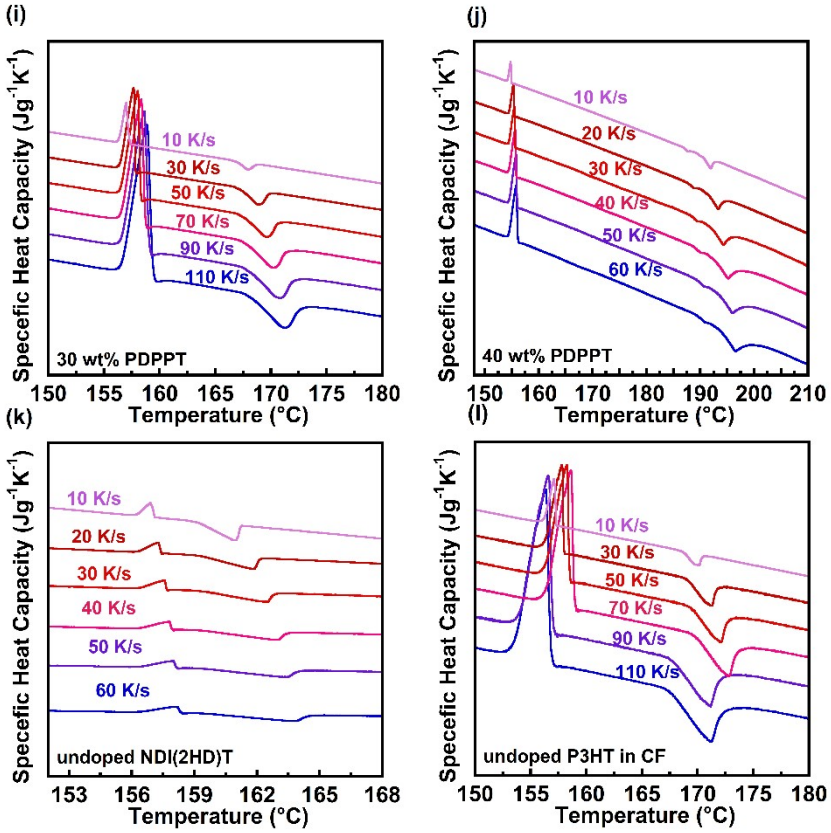

Figure S2. Representative Flash DSC scans for thermal lag vs. temperatures **a)** 1 wt% doped P3HT **b)** 5 wt% doped P3HT **c)** 10 wt% doped P3HT **d)** 20 wt% doped P3HT **e)** 1 wt% doped PDPPT **f)** 5 wt% doped PDPPT **g)** 10 wt% doped PDPPT **h)** 20 wt% doped PDPPT **i)** 30 wt% doped PDPPT **j)** 40 wt% doped PDPPT **k)** undoped NDI(2HD)T **l)** undoped P3HT processed from chloroform solvent.

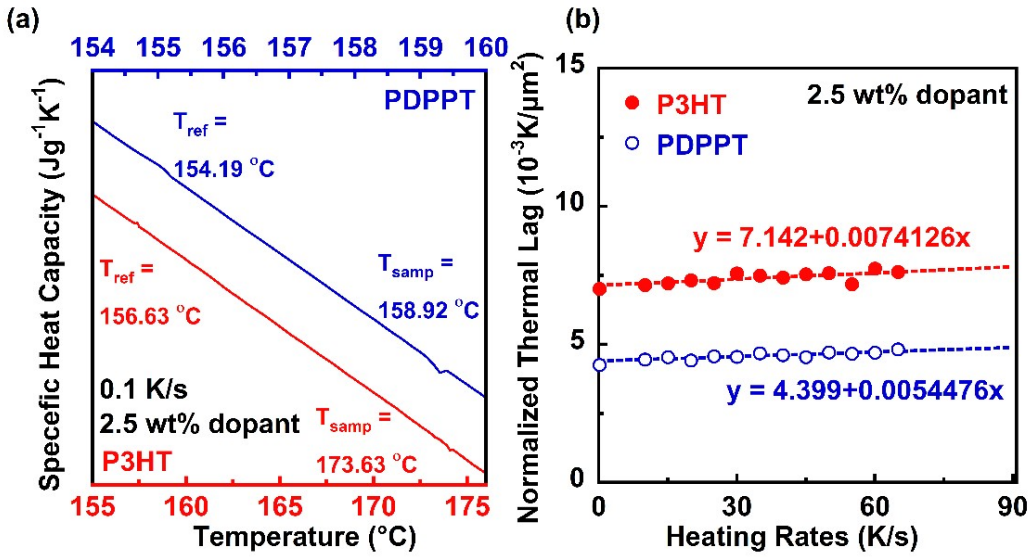

Figure S3. a) The melting temperature for reference Indium (T_{ref}) and sample Indium on the top of testing film (T_{samp}) at heating rate of 0.1 K/s. **b)** normalized thermal lag vs. heating rates plot for 2.5 wt% doped P3HT and PDPPT, where dashed lines are based on the linear fitting equations for heating rates from 10 to 65 K/s.

$\Delta T_{m,P3HT}$ = 17.0 K; h_{P3HT} = 49.24 μm; normalized thermal lag = 7.01*10^{-3} K/μm^2

$\Delta T_{m,P3HT}$ = 4.73 K; h_{P3HT} = 33.37 μm; normalized thermal lag = 4.25*10^{-3} K/μm^2

Those two points are quantitatively captured by the fitting equations which are based on the heating rates from 10 to 65 K/s (as shown in **Figure S3b**). Therefore, based on the thermal transport, there will be a temperature difference between bottom and top surfaces no matter how low the heating rate is.

The initial thermal lag is due to the temperature gradient between chip membrane and the top film. Thus, the thicker film showed larger initial thermal lag if the thermal conductivity were comparable. It clearly showed that the dominant factor for the initial thermal lag is film thickness rather than the interfacial thermal resistivities, as shown in the following table.

Table S1. The initial thermal lag for selected doped P3HT and PDPPT Samples

	Dopant wt%	Thickness (nm)	Initial Thermal lag (°C)
P3HT	1.0	21.9	4.83
	2.5	49.24	17.3
PDPPT	1.0	22.08	2.2
	2.5	33.37	4.90

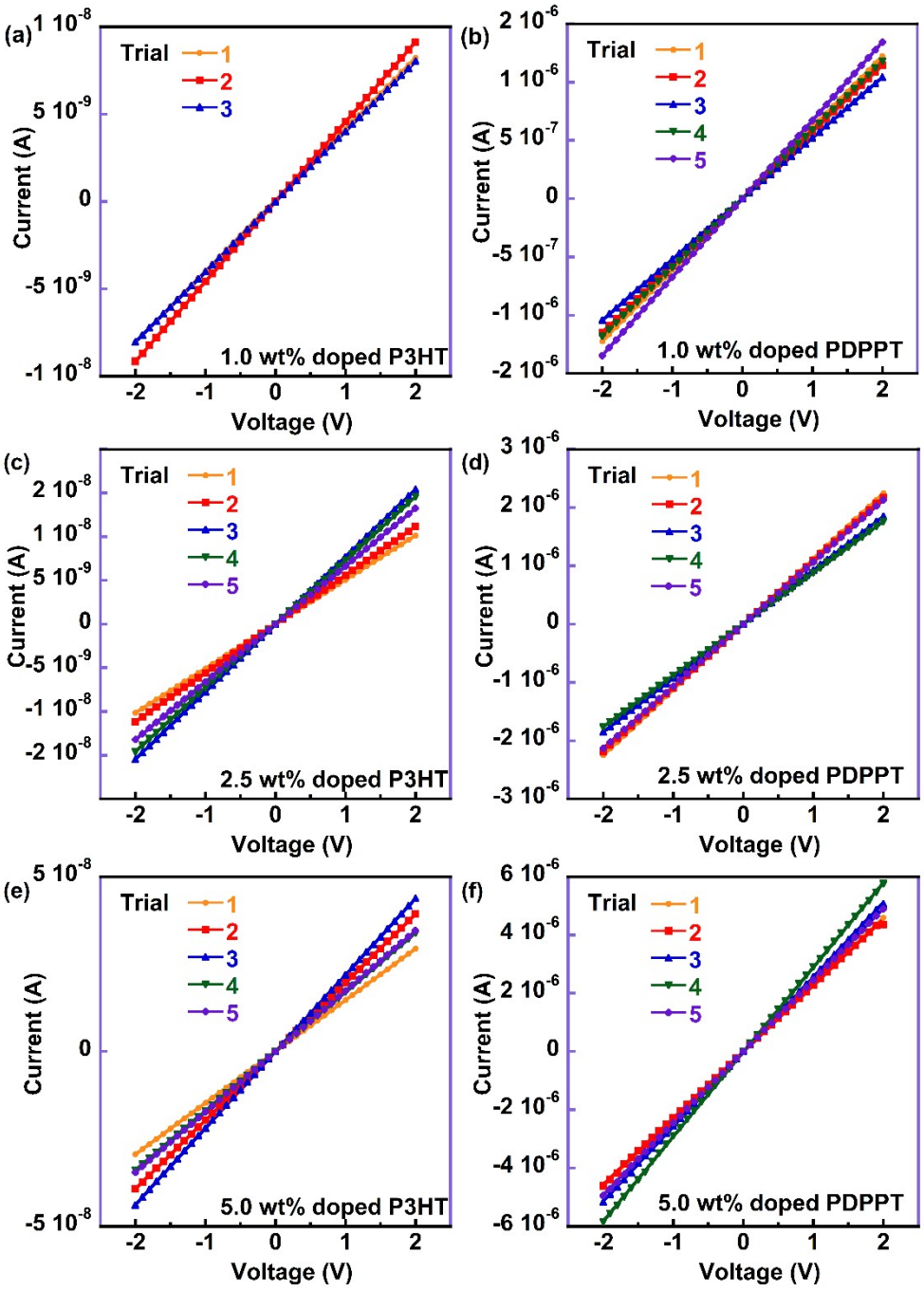

Figure S4. Voltage vs. current scan curves for **a)** 1.0 wt% P3HT doped films, **b)** 1.0 wt% PDPPT doped films, **c)** 2.5 wt% P3HT doped films, **d)** 2.5 wt% PDPPT doped films, **e)** 5 wt% P3HT doped films **f)** 5 wt% PDPPT doped films

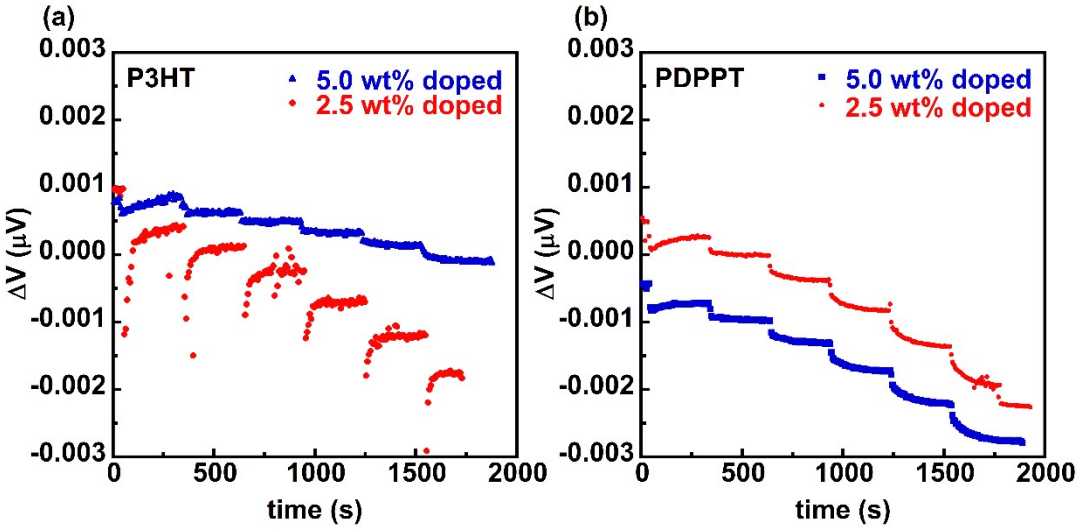

Figure S5. Seebeck coefficient for a) P3HT and b) PDPPT doped films.

*The raw data are only available for measurement manually using a voltage-sourced two-point probe method and peltier devices, respectively. For the rest of the doping concentrations, measurements were performed on Netzsch SBA 548 Nemesis thermoelectric set up under an He environment at room temperature by the 'test option' in the instrument.

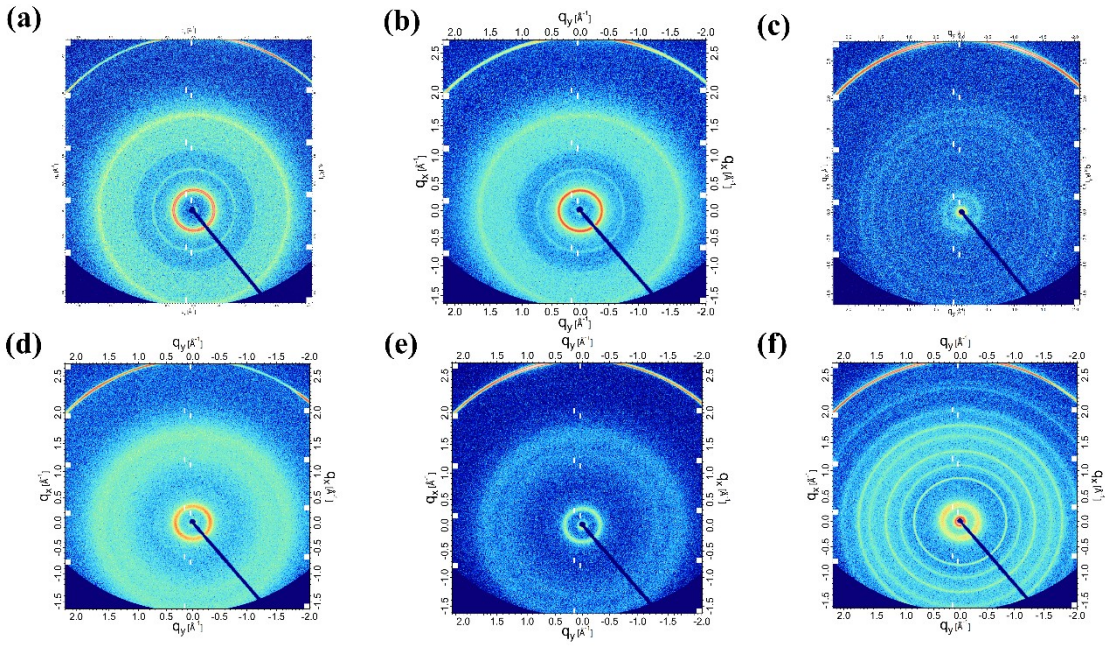

Figure S6. 2D WAXS images for P3HT dropcast films **a)** 5 wt%, **b)** 10 wt%, **c)** 30 wt%, PDPPT dropcast films **d)** 5 wt%, **e)** 10 wt%, **c)** 40 wt%

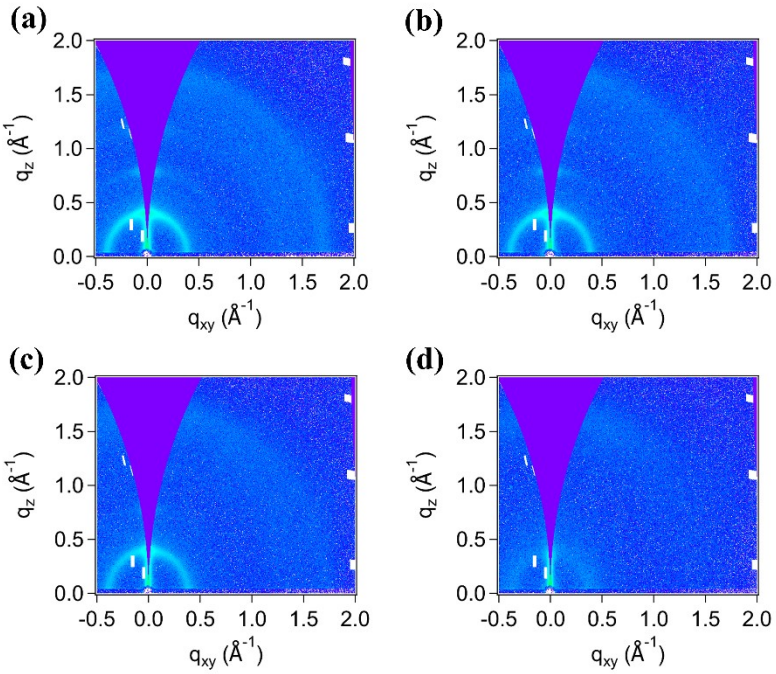

Figure S7. 2D GIWAXS images for **a)** undoped, **b)** 5 wt%, **c)** 10 wt%, **d)** 20 wt%

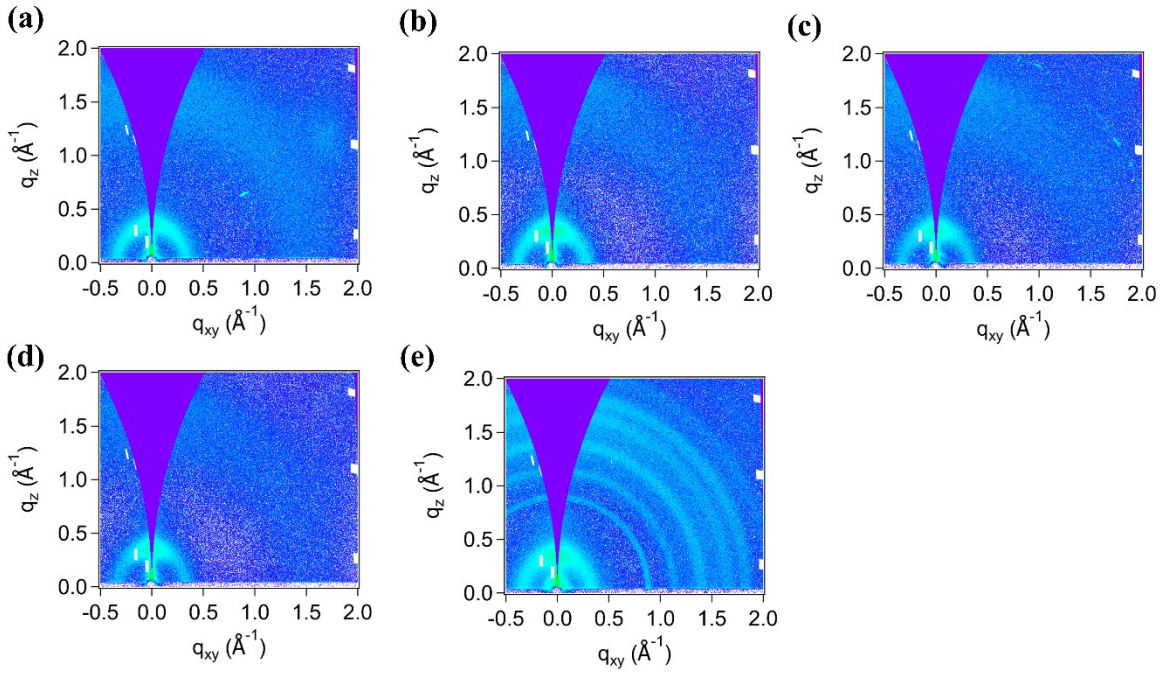

doped P3HT films

Figure S8. 2D GIWAXS images for **a)** undoped, **b)** 5 wt%, **c)** 10 wt%, **d)** 20 wt%

doped, **e)** 40 wt% doped PDPPT films

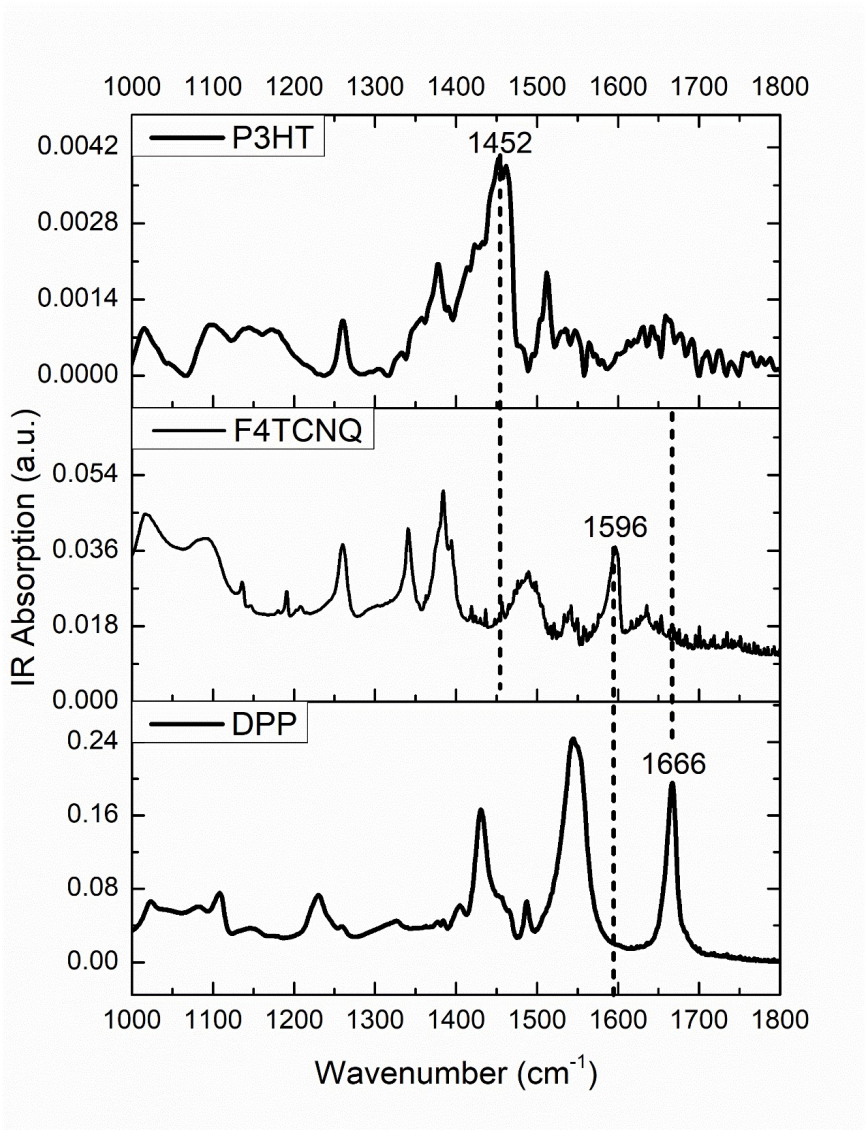

Figure S9. FTIR absorbance spectrum of P3HT, F4TCNQ, and PDPPT

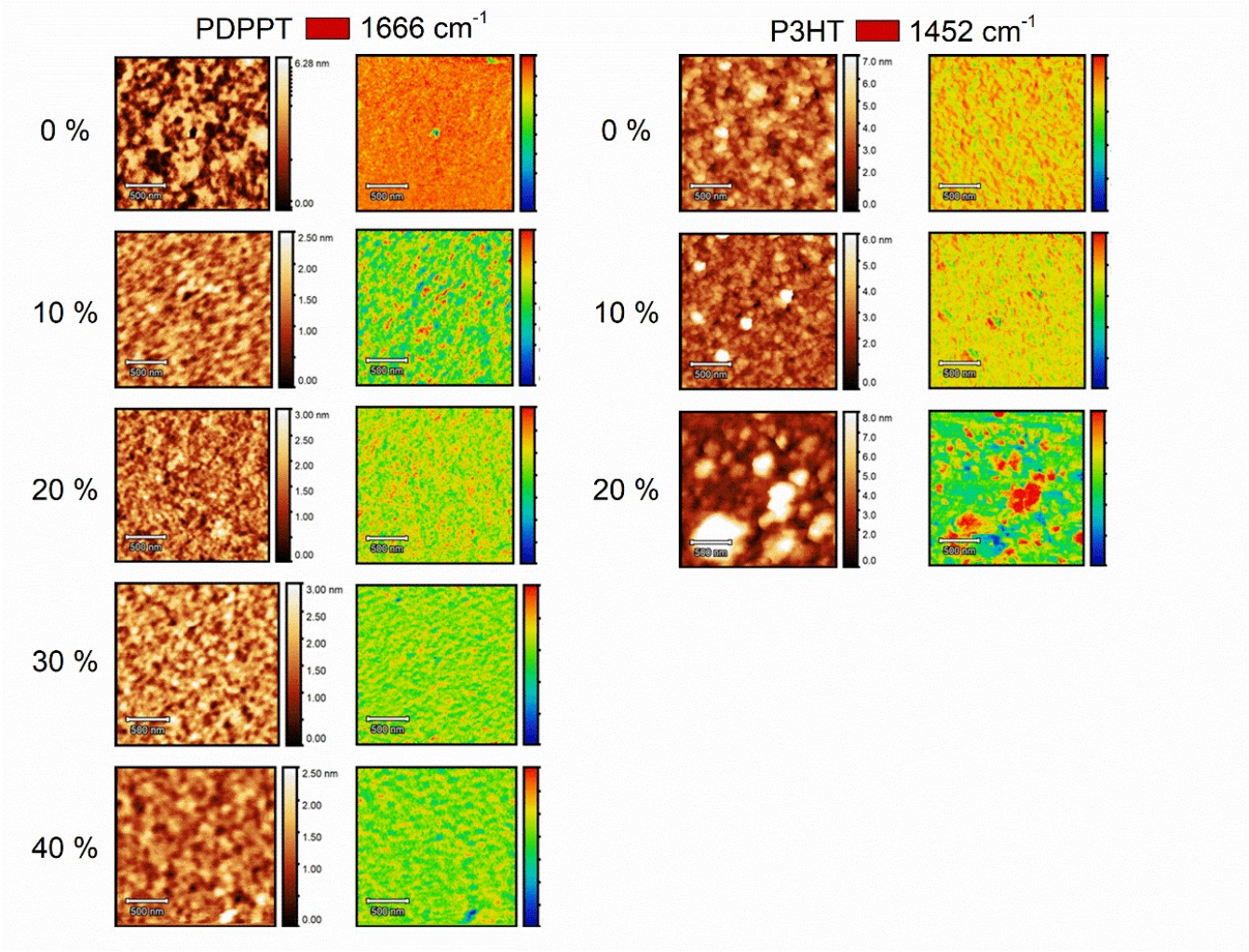

Figure S10. Additional AFM-IR images for PDPPT and P3HT doped films ranging from 0 to 40 % doped for PDPPT and 0 to 20 % for P3HT.

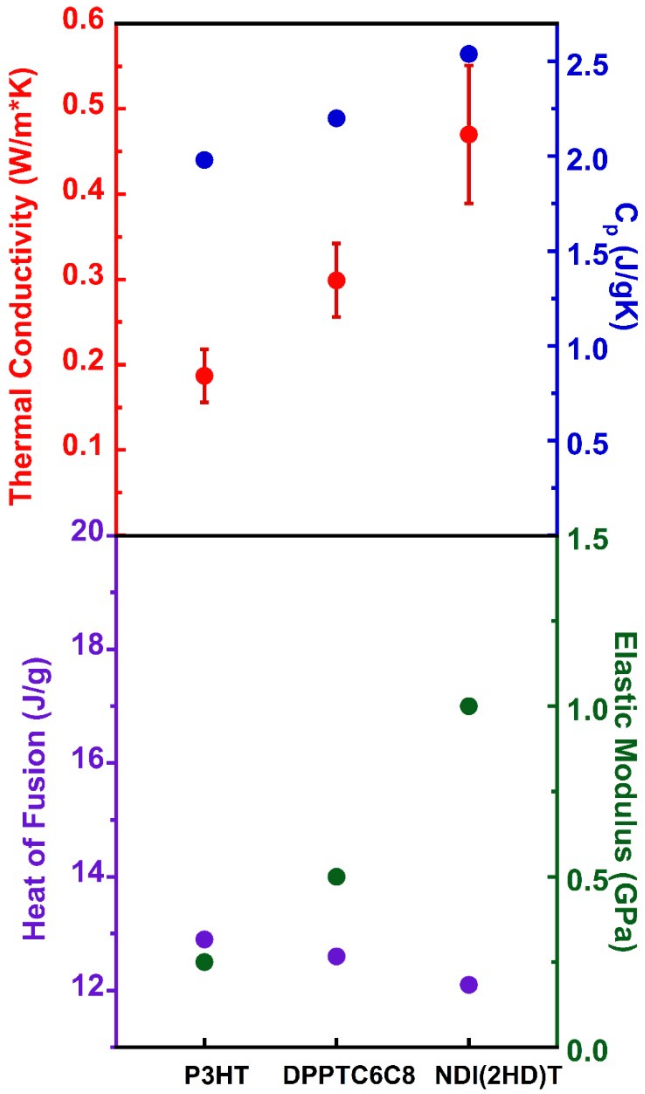

Figure S11. Thermal conductivity (red circle), heat of fusion (purple circle), specific heat capacity (blue circle) and elastic modulus (green circle) plotted against three different conjugated polymers, P3HT, DPPT and NDI(2HD)T, respectively.

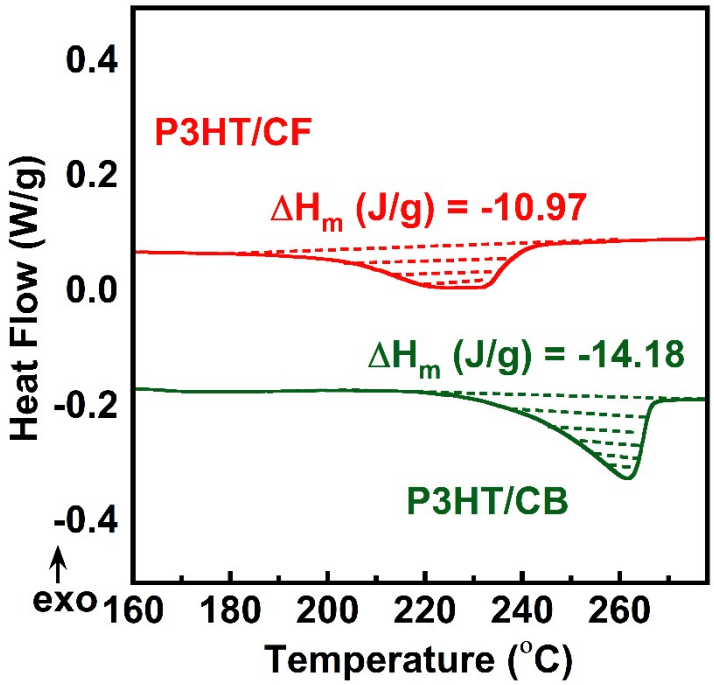

Figure S12. Melting peaks from first scan for P3HT dissolved in chlorobenzene (P3HT/CB) and P3HT dissolved in chloroform (P3HT/CF)

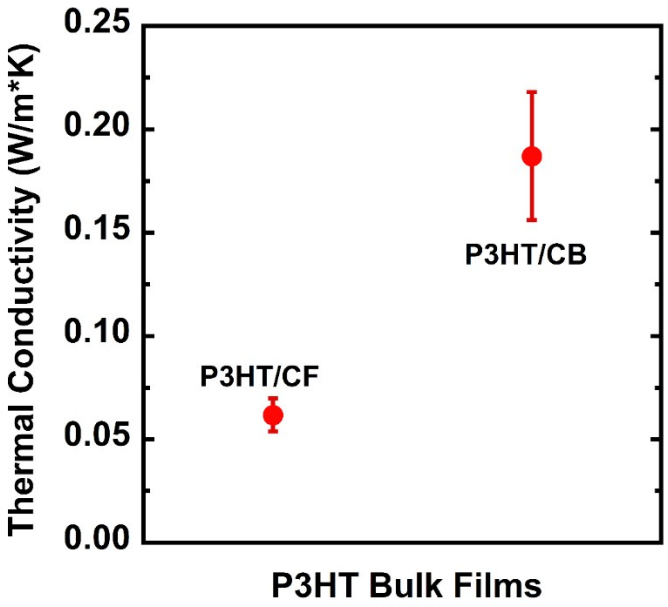

Figure S13. Thermal conductivity for undoped P3HT films dissolved in different chloroform (CF) and chlorobenzene (CB), respectively.

Electronic contributions for thermal conductivity for doped films

In this work, the dopant enhanced charge carrier mobility/concentrations for CPs. To quantitatively investigate the amount of conductivity contributed by improved charge carrier mobility, the Wiedemann-Franz Law (WFL), as $K_E = L\sigma T$, is introduced and used here, where L is Lorenze number that equals Sommerfeld number[1] (L_0 = 2.45*10^{-8} WΩK^{-2}). Using this empirical equation, we estimated that a 0.1 W/mK enhancement in thermal conductivity would require a substantial increase in electrical conductivity of 100 S/cm at the experimental temperature of 429 K. Nonetheless, the highest electrical conductivity measured in this work is only 0.4 S/cm for the 20 wt% doped P3HT films, therefore, free electrons are not expected for the main reason for the observed thermal conductivity enhancement upon doping since the highest K_E will be 0.0004 W/mK.

Instrument Intrinsic Thermal Lag

It is important to validate our method to ensure it quantifies the thermal property

correctly. First, we confirmed thermal lags used to calculate the thermal conductivity are originated from the testing CP films instead of the instrumental intrinsic thermal lags. Three experiments were performed for the sole indium placed on the sample side substrate to estimate the intrinsic thermal lag for instruments, as discussed in literature[2]. The melting peak of single indium increased as heating rates increased, as shown in **Figure 14a**. The dashed lines are the following fitting equation:

$$T_{measured} = T_{initial} + \beta(m_{In} * \tau_m + 0.2\ ms) \quad (1)$$

where $T_{initial}$ is the initial melting temperature of indium, m is the calculated mass of 0.67 μg of single indium, τ_m is the thermal lag time constant and 0.2 ms time lag was reported for the low-stress silicon-nitride thin membrane of Flash DSC chip[1]. From fitting slopes, the averaged τ_m is 2. 86 ms/μg (τ_{m1}=3.0 ms/μg, τ_{m2}=2.9 ms/μg, τ_{m3}=2.7 ms/μg, respectively). Considering that the indium samples used in this work were less than 0.4 μg, the overall intrinsic thermal lag was 1.2 ms, which was negligible compared to the actual experiment time scale (0.5s to 5s). Therefore, we can conclude that thermal lags between indium and substrate is negligible.

Reliability and Reproducibility Test

In addition to intrinsic thermal lag, the silicon oil should be applied to both testing CP films and Flash DSC chips. To ensure no interactions between CP films/silicon oil/Flash DSC chips, we have performed reliability/repeatability tests, where multiple heating/cooling cycles (a complete temperature program shown in **Figure 1b** counted as one cycle) are conducted for the same sample. The unchanged melting peaks for sample indium and reference indium confirmed the good reproducibility and reliability for this method and we assured that there were no interactions between CP films and silicon oil (representative plot shown in **Figure**

S14b).

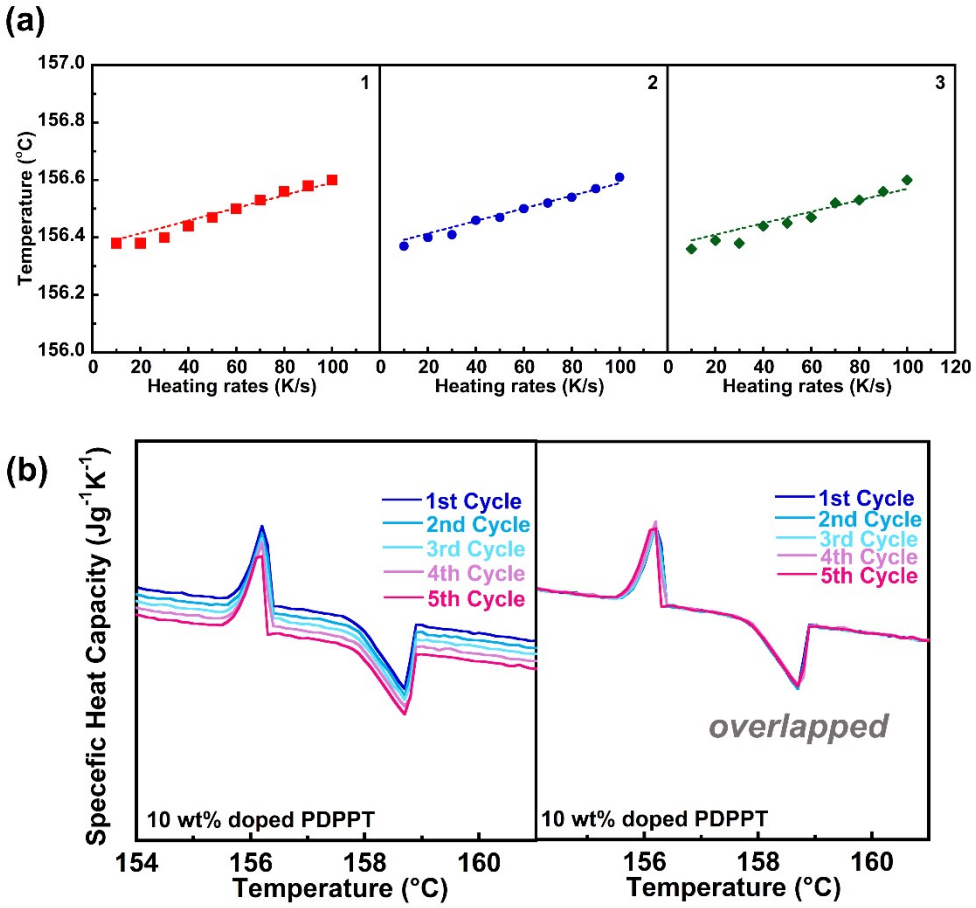

Figure S14. a) Three measurements for melting temperature for single indium placed on sample side only, where dashed lines are fitting results from Equation 6 **b)** thermal lag plots for 10 wt% doped PDPPT, where each cycle represent a whole temperature program from 10 to 60 K heating/cooling process.

Reference:

1. G. S. Kumar, G. Prasad and R. O. Pohl, J. Mater. Sci., 1993, 28, 4261–4272.
2. Van Herwaarden, S.; Iervolino, E.; Van Herwaarden, F.; Wijffels, T.; Leenaers, A.; Mathot, V. Design. Thermochim. Acta **2011**, *522* (1–2), 46–52.

Table S2. Statistical analysis for thermal conductivity measurement

sample name	Thickness, h (μm)	Density, ρ (g/cm^3)	Specific Heat Capacity, C_p (J/gK)	Slope, dT/dβ (K/s)
5 wt% doped PDPPT	33.42 ± 0.24	1.01	2.2	$(5.92 \pm 0.53)*10^{-3}$

$$K = \frac{h^2 \rho_{film} C_{p,film}}{\frac{dT}{d\beta}} = \frac{2.2 * (1.01 * 10^6)(33.42 * 10^{-6})^2}{5.92 * 10^{-3}} = 0.420\ W/mK$$

$$U\{K\} = K * \sqrt{[\frac{U(h)}{h}]^2 + [\frac{U(h)}{h}]^2 + [\frac{U\left(\frac{dT}{d\beta}\right)}{\frac{dT}{d\beta}}]^2} = \frac{2.2}{}$$

$$= 0.038\ W/mK$$

Thus, the uncertainty for the measurement in this work for 5 wt% doped PDPPT is 0.037 W/mK. Thus we conclude that K = (0.420 ± 0.038) W/mK

Table S3. 3ω method by Linseis TFA for doped PDPPT thermal conductivity

Temperature / ˚C	10 wt% doped PDPPT (W/mK)
24.75	0.37
39.75	0.37
54.75	0.37
69.75	0.37
84.75	0.37
99.75	0.38
114.75	0.39
129.75	0.40